Micromachines for Microchips: Bringing the AFM up to Speed

March 20, 2000
Scientific and Technical Final Report

NanoDevices Inc., 516 E. Gutierrez, Suite E., Santa Barbara, CA 93103
805-884-0240, 805-884-0540 (Fax), steve@ndevices.com

PI: Stephen C. Minne, Ph.D.

DTIC QUALITY INSPECTED 1

20000411 106

REPORT DOCUMENTATION PAGE

Form Approved
OMB No. 0704-0188

1. REPORT DATE *(DD-MM-YYYY)*	2. REPORT TYPE	3. DATES COVERED *(From - To)*
27-03-00	Final Report	Oct. 1999 – Apr. 2000

4. TITLE AND SUBTITLE

Micromachines for Microchips:
Bringing the AFM up to Speed

5a. CONTRACT NUMBER
DAAH01-00-C-R014

5b. GRANT NUMBER
PAN RTW 26-00

5c. PROGRAM ELEMENT NUMBER

6. AUTHOR(S)

Minne, Stephen, C, Ph.D.

5d. PROJECT NUMBER

5e. TASK NUMBER
Sequence A002

5f. WORK UNIT NUMBER

7. PERFORMING ORGANIZATION NAME(S) AND ADDRESS(ES)
NanoDevices, Inc.
516 E. Gutierrez, Suite E
Santa Barbara, CA 93103

8. PERFORMING ORGANIZATION REPORT NUMBER

9. SPONSORING/MONITORING AGENCY NAME(S) AND ADDRESS(ES)

Defense Advanced Research Projects Agency

10. SPONSOR/MONITOR'S ACRONYM(S)

AMSAM-RD-WS-DP-SB

11. SPONSOR/MONITOR'S REPORT NUMBER(S)

12. DISTRIBUTION/AVAILABILITY STATEMENT

Distribution Unlimited

13. SUPPLEMENTARY NOTES

14. ABSTRACT   This Phase I SBIR final report, developed under contract for topic number DARPA SB992-039, outlines improvements made to the atomic force microscope (AFM) in order to increase its imaging speed 50 to 100 times in the contact mode. Faster imaging will allow the AFM to be used in high throughput military and microelectronic manufacturing applications. The crux of the effort is to eliminate the rate-limiting element of the conventional AFM: the piezoelectric z-axis tube actuator. This actuator is typically large, and therefore slow (about 600 Hz resonance). In this work the bulk actuator is replaced by one fabricated (using microelectronic processes) directly onto the microscope's cantilever. The new actuator is much smaller, and therefore much faster (60 kHz resonance). When integrating the actuator directly onto the cantilever, the dynamics of the sensing instrumentation are changed. This change is corrected with a high-speed electronic circuit. Likewise, the remaining circuitry within the microscope must be modified to accommodate the faster signals. Atomic force microscope images taken 50 to 100 times faster are presented. This speed improvement allows atomic scale video rate imaging.

15. SUBJECT TERMS
SBIR Report, Atomic Force Microscopy, High Speed Atomic Force Microscopy, AFM, Scanning Probe Microscopy, SPM

16. SECURITY CLASSIFICATION OF:			17. LIMITATION OF ABSTRACT	18. NUMBER OF PAGES	19a. NAME OF RESPONSIBLE PERSON
a. REPORT	b. ABSTRACT	c. THIS PAGE			*, Stephen C. Minne
U	U	U	UU		**19b. TELEPHONE NUMBER** *(Include area code)* 805-884-0240

Standard Form 298 (Rev. 8/98)
Prescribed by ANSI Std. Z39.18

Summary

The objective of this project is to develop an atomic force microscope (AFM) platform capable of high speed imaging in the contact and the intermittent contact modes of operation. The AFM is a unique tool for surface characterization because is it capable of producing three dimensional atomic scale images. As features on advanced electronics and data storage devices continue to shrink, obtaining high resolution measurements on these surfaces grows in importance. For these applications, traditional forms of metrology have been stretched to their limits. Standard optical microscopes are fundamentally limited by optical diffraction to around 100 nm. The scanning electron microscope (SEM) can provide nanometer scale resolution, but it does not produce three dimensional data. The AFM provides the necessary information with the necessary resolution, however it is not fast enough to be used in production applications. By analyzing the operation of the AFM, this research effort succeeded in reaching the project's goals of increasing the throughput of the AFM by 30 times. In contact mode imaging this was accomplished by replacing the AFM's feedback actuator (an element which is normally the size of one's finger) with a micromachined device that is only a fraction of a millimeter long. For intermittent contact mode imaging, the speed was increased by using the previous technique coupled with an active filter that simulates viscous drag. All solicited and proposed objectives were met or exceeded. Images using high speed AFM imaging in the contact and intermittent contact mode are presented.

Table of Contents

Introduction

The ever-expanding military demands on the microelectronics, data storage, and biological industries require advancements in technology that are broad-based and crosscutting. Recently, the primary advances in these fields have come through system miniaturization. Advancements through miniaturization have placed a premium on high-resolution surface inspection and imaging. For many applications in these fields, the capabilities of traditional imaging techniques have been stretched to their limits. A robust high-speed high-resolution inspection tool is needed for continued miniaturization and enhanced functionality in these areas.

The atomic force microscope (AFM) was invented in 1986, and has since gained much popularity in high-resolution three-dimensional imaging. A schematic diagram of a typical AFM is shown in Figure 1. The AFM can be used in a wide variety of modes, including fluid imaging, magnetic imaging, capacitive imaging, and thermal imaging. However, the AFM has found its main use in high-resolution surface characterization. The two dominant AFM modes for surface characterization are the contact mode and the intermittent-contact mode.
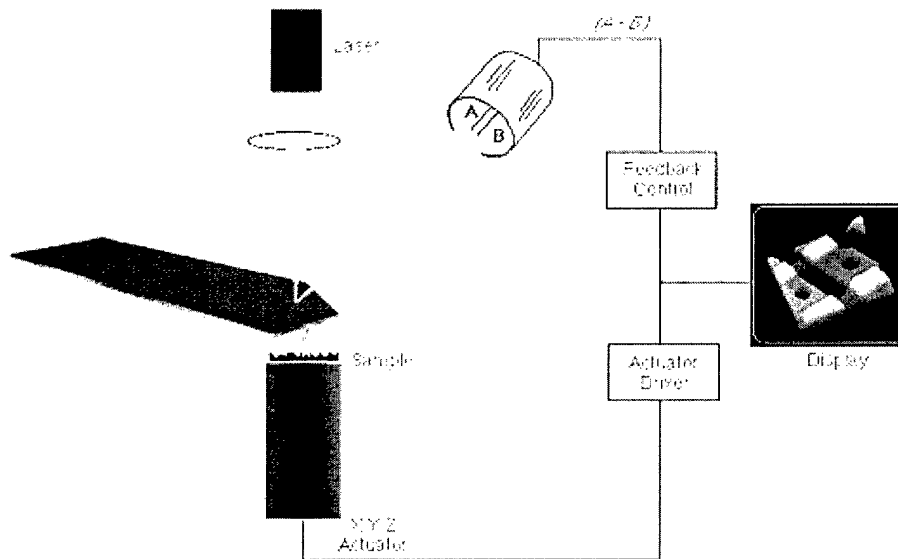
Figure 1: A schematic of a typical Scanning Probe Microscope (SPM). A image is formed by using the laser/cantilever/detector system to measure the height of every pixel of an image.

In the contact mode, the AFM operates by scanning an atomically sharp tip mounted on soft flexible cantilever across the surface to be imaged. As topographic features on the sample pass under the sharp tip, they cause the flexible cantilever to deflect. A sensor within the microscope monitors the deflection of the cantilever, recording the height of each pixel in the image. Since the raster scan is input by the user, the lateral position can be fed into a computer along with the measured height data, and a three-dimensional image of the surface can be rendered.

Typically, the contact mode AFM is operated in closed loop feedback. The feedback loop monitors the deflection of the cantilever and adjusts the sample position in

4

order to keep the forces between the tip and the sample constant. Maintaining a constant tip sample force preserves the delicate tip and protects fragile samples.

An intermittent contact mode microscope is very similar to the contact mode microscope. For intermittent contact imaging, two additional components are added to the schematic in Figure 1 (not shown). First, a small piezoelectric stack is placed under the cantilever, and second, an RMS to DC converter is placed after the split photodiode. During imaging, the cantilever is oscillated at its resonant frequency by the piezoelectric stack. As the tip rasters over the sample, the topographic data is obtained by measuring the degree to which the sample impedes the cantilever's oscillatory motion through the RMS to DC converter. Like in the contact system, feedback is used to move the sample relative to the tip to maintain a constant tip sample interaction. Otherwise the drivers, the electronics, and the actuators are the same as in the contact mode system. Intermittent contact mode imaging is the preferred method for AFM imaging because it eliminates lateral forces between the tip and the sample. (This mode of imaging is often referred to as Tapping Mode ™, a trade name from Digital Instruments of Santa Barbara, CA.) Elimination of the lateral forces enhances the AFM's image fidelity and preserves the cantilever's tip sharpness.

As features on functional devices continue to shrink, the ability to monitor nanometer scale features "in-line" becomes more important. The AFM has demonstrated its ability to monitor these small features, however its slow speed prevents it from being widely accepted as an "in-line" tool. Currently, AFM images take several minutes to obtain. The speed of imaging depends on the mode of operation, but is generally limited by one of two fundamental parameters. In contact mode feedback imaging, the bandwidth of the feedback loop is the rate limiting parameter. In most AFMs, the speed of the feedback loop is generally limited by the speed of the feedback actuator. In the intermittent contact mode, the feedback loop is still a limiting factor, but no longer the dominant factor. For a typical AFM operating in the intermittent-contact mode, the rate limiting parameter is the speed at which the resonating cantilever can increase its amplitude. This speed is related to the width of the resonant peak, or the cantilever Q. These limitations typically restrict the AFM's imaging bandwidth to 1 kHz in the contact mode and 300 Hz in the intermittent-contact mode.

This research addressed these imaging speed issues by focusing on the fundamental limiting factors of the AFM: 1) the z-axis actuator resonance, and 2) the Q of the oscillating cantilever.

The current z-axis actuator in most AFM systems is typically a bulk piezo-tube about the size of one's finger. Large items typically have very low resonant frequencies, and the typical piezo-tube's first resonance occurs between 600 Hz and 1 kHz. Removing the piezotube from the feedback system can solve this limitation. However the functionality of the actuator is still needed to operate in the feedback mode, so rather than eliminate it completely, in this work it is replaced with a small micromachined actuator integrated onto the cantilever. Because this new actuator is very small it is very fast. The data shows that the micromachined actuator will increase the bandwidth of the AFM by a factor of 100 without losing sensitivity, or total actuator movement.

The width of the resonance of the oscillating cantilever limits the imaging speed because it determines the rate at which energy can be added to (or dissipated from) the cantilever system. For example, if the cantilever has a very high Q (or narrow width),

5

very little mechanical energy can be added per cycle. If the cantilever travels off a step edge, it will take a finite time for the cantilever to "ring" up to its full amplitude. This ring up time determines the free cantilever bandwidth, and has a time constant of Q/w_o. To address this problem, we used a system where the integrated actuator is used to actively damp the oscillations of the cantilever (in addition to adjusting tip/sample spacing).

Phase I Objectives

The overall objective of the proposal was to develop a commercially viable system for very high speed atomic force microscopy in the contact and the intermittent contact mode. The system should be relevant to research, manufacturing, and production applications. These specific objectives were enumerated in the Phase I proposal as follows:

Contact Mode:
1) Design and implement a feedback loop capable of stable operation in a 20 kHz bandwidth.
2) Design and implement a piezoelectric angle induced deflection correction circuit capable of stable operation in a 20 kHz bandwidth.
3) Demonstrate proof of concept of the topic's goal by measuring a 1 to 2 order of magnitude improvement in contact mode's closed loop transfer function.
4) With the transfer function, quantify speed benefits over a conventional system and describe the new performance limits.

Intermittent Contact:
5) Design and implement the electronics and mechanics necessary for actively damping, or enhancing, an AFM cantilever's resonance.
6) Using item 5, in addition to the contact mode enhancements (specifically item 1), demonstrate proof of concept of the topic's goal by measuring a 1 to 2 order of magnitude improvement in the intermittent contact mode's closed loop transfer function.
7) With the transfer function, quantify speed benefits over a conventional system and describe the new performance limits.

Overall Status & Work Performed

A new procedure for high speed imaging with the atomic force microscope that combines an integrated ZnO piezoelectric actuator with an optical lever sensor has yielded an imaging bandwidth of 33 kHz. This bandwidth is primarily limited by a mechanical resonance of 77 kHz when the cantilever is placed in contact with a surface. Images scanned with a tip velocity of 1 cm/s have been obtained in the constant force mode by using the optical lever to measure the cantilever stress. This is accomplished by subtracting an unwanted deflection produced by the actuator from the net deflection measured by the photodiode using a linear correction circuit. Additionally, a flexible

6

system for increasing the throughput of the atomic force microscope without sacrificing imaging range is presented. The system is based on a nested feedback loop which controls the micromachined cantilever that contains both an integrated piezoelectric actuator and an integrated thermal actuator. This combination enables high speed imaging (2 mm/s) over an extended range by utilizing the piezoelectric actuator's high bandwidth (15 kHz) and thermal actuator's large response (300 nm/V). For both high speed contact mode configurations, constant force images are presented

The speed of tapping mode imaging with the atomic force microscope (AFM) has been increased by over an order of magnitude. The enhanced operation is achieved by 1) increasing the instrument's mechanical bandwidth and 2) actively controlling the cantilever's dynamics. The instrument's mechanical bandwidth is increased by an order of magnitude by replacing the piezotube z-axis actuator with an integrated zinc oxide (ZnO) piezoelectric cantilever. The cantilever's dynamics are optimized for high-speed operation by actively damping the quality factor (Q) of the cantilever. Active damping allows the amplitude of the oscillating cantilever to respond to topography changes more quickly. With these two advancements, 80 μm x 80 μm high speed tapping mode images have been obtained with a scan frequency of 15 Hz. This corresponds to a tip velocity of 2.4 mm/s.

Details of the experimental configurations are described in the following sections. These results meet or exceed all of the solicited and proposed objectives.

Technical Description:
Contact Mode Imaging

The atomic force microscope (AFM) has become an essential instrument for visualizing, monitoring, and characterizing surfaces. Since its introduction in 1986 there has been a steady stream of innovations which have increased the sensitivity and functionality of the instrument. Current state of the art for AFMs can now map topography, friction, electric, and magnetic fields, temperature, and more. When imaging, vertical resolutions of less than 1A are routinely achieved. However, for most AFMs, the throughput, or the time it takes to acquire an image, has not improved. Recently, there has been effort in increasing the throughput of scanning probe microscopy.[1,2,3] However, throughput increases cannot come at the expense of resolution or tip wear. For contact mode imaging, this requires that the probe maintains a constant force on the sample.[4] For most AFMs, the maximum scan rate at which the contact mode can operate is limited by the bandwidth of the actuator responsible for providing constant force. Typically, the actuator consists of a macroscopic piezoelectric material in the form of a tube or stack which exhibits relatively low resonant frequencies (often less than 1 kHz). This can limit scanning speeds to less than a few hundred microns per second. As a result, it often takes minutes to produce a single image.

Previously, it was found that the scan speed of the contact mode AFM could be increased an order of magnitude by integrating a thin layer of ZnO on the base of a piezoresistive cantilever.[5] The cantilever was bent to follow sample topography by applying a voltage across the ZnO while the sample force was detected by measuring the piezoresistor. In that study, both the imaging bandwidth (6 kHz) and the resolution (~60

Å) were limited by complications in measuring the piezoresistor. We expect that these results could be improved by optimizing the cantilever design and refining the detection electronics. However, the susceptibility to unwanted electrical interference of a detector consisting of an electrical loop near the piezoelectric actuator can make it difficult to obtain large bandwidths with high resolution.

We report here the extension of high speed imaging with an integrated actuator to include an optical lever sensor. This was reported by Manalis et.al. in conjunction with the author at Stanford University.[6] The optical lever, developed by Amer and Meyer,[7] and Alexander et al.[8], is capable of sub-angstrom vertical resolution and is not influenced by electrical signals that control the integrated actuator.

Referring to figure 1, in a standard system, constant tip/sample force is achieved by translating either the cantilever or the sample with a servo loop that maintains a constant cantilever deflection. The optical lever is used to measure the deflection angle of the cantilever. In ordinary circumstances, this angle only changes when a force is acting on the tip. Thus the optical lever gives a true measure of the force. In a system where the actuator is mounted on the cantilever, motion in the vertical direction is achieved by changing the angle of the cantilever[9] and this is a problem that must be addressed when the optical lever is used for detection. This scheme is depicted in Figure 2 for three cases where: (a) the tip/sample force is near zero, (b) the cantilever is strained by a topographical step, and (c) a voltage is applied to the ZnO to relieve the strain. The angle of the reflected beam in (a) is different from the angle in (c) although the force is the same. In this configuration, the signal measured by the optical lever is a function of the ZnO bending in the absence of a force on the tip. It is a simple matter to construct a circuit that subtracts this unwanted signal from the servo loop. We have found that a first order linear correction applied to a 720 μm long cantilever yields a vertical range where constant force is possible. Using this correction procedure, we present a 100 μm x 100 μm image scanned with a tip velocity of 1 cm/s, as well as a high resolution image of the granular structure of gold scanned at 0.5 mm/s. In the case of the high resolution image, the tip speed was limited by the scanning device.
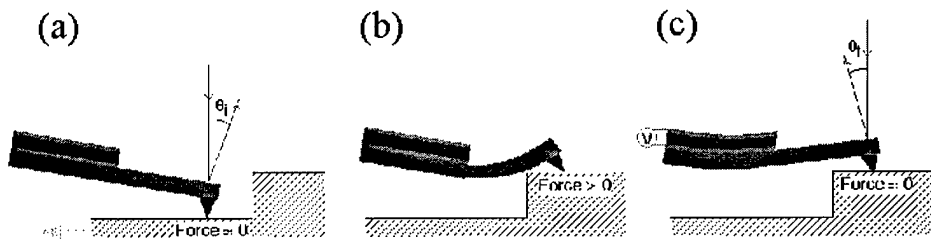

Figure 2: Schematic diagram showing the effects of integrated actuator's induced angle. (a) The initial cantilever shape, (b) the shape after being scanned over a step, and (c) the shape after an appropriate voltage is applied to the ZnO to return the cantilever stress to that shown in (a). The cantilever exerts an equal force on the sample in (a) and (c) but the deflection angle of the laser beam is the same. The difference, created by the actuator itself, can be subtracted from the photodiode signal so that only strain induced bending of the cantilever is measured.

A schematic of the high speed contact mode atomic force microscope (AFM) is shown in Figure 3. The silicon cantilever can be displaced vertically up to 4 μm using a layer of ZnO located at the cantilever base.[10] To maximize the displacement for a given

applied voltage, the ZnO thickness is 3.5 μm and is equal in thickness to the silicon portion of the cantilever. Because the spring constant is proportional to the thickness cubed, and the base is twice as thick as the remainder of the cantilever, most of the bending will occur in the thinner portion when the tip is deflected. Therefore we can effectively uncouple the deflection of the cantilever caused by applying a voltage across the ZnO and the deflection caused by physically displacing the tip with a sample. As a result, if the tip is in contact with a surface while the ZnO voltage is modulated, the deflection signal from the photodiode will consist of two angular components: the strain-induced angle (depicted in Figure 2b), and the ZnO-induced angle (Figure 2c). To obtain constant force, the servo loop must detect only the strain-induced angle.
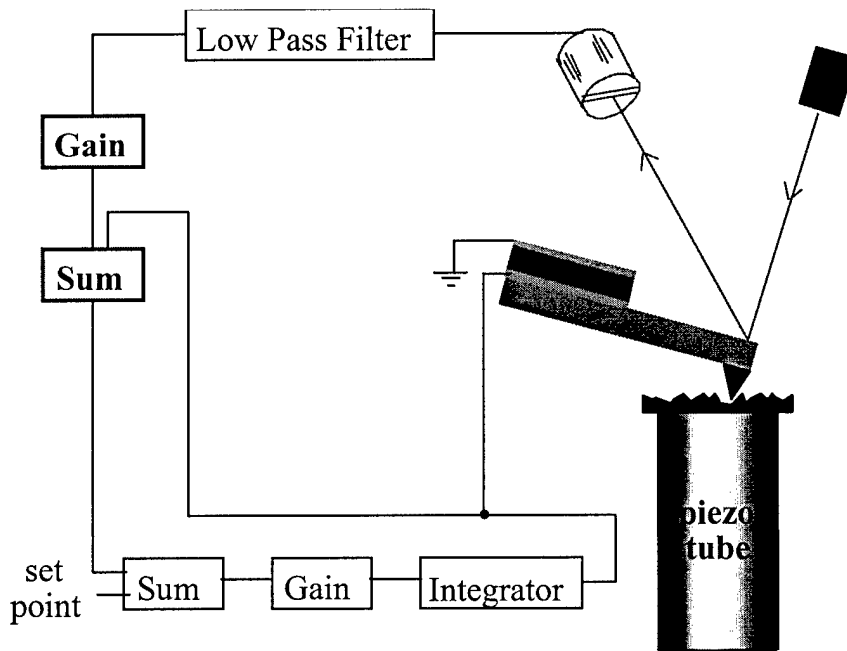

Figure 3. Atomic force microscope schematic including a linear correction of the photodiode used to remove the ZnO induced bending.

To eliminate the ZnO-induced angle, we sum the output of the photodiode with the signal that controls the ZnO (see Figure 3). In order to calibrate the correction scheme, the ZnO is modulated while the tip end of the cantilever is free and the gain of the photodiode output is adjusted so that the corrected deflection is nulled. At this point, the servo loop cannot distinguish between the scenario depicted in Figures 2a and 2c.

The frequency response of the actuator, sensor, and servo loop is determined by modulating the setpoint while the tip is in contact with a surface (see Figure 3). First, the integral gain and time constant of the servo loop are increased to just below the point where the system becomes unstable. The modulation frequency of the setpoint is then swept while the output of the integrator (ZnO signal) and input to the gain/integrator (error signal) are recorded. The amplitude and phase response of the ZnO are shown in Figure 4a, and the error signal is shown in Figure 4b for a 570 μm long cantilever. By adding a 12 dB low pass filter at 100 kHz, we could increase the integral gain while still maintaining stability of the servo loop. The resulting bandwidth is 33 kHz for a 45 degree phase shift of the error signal. The mechanical resonance at 77 kHz (shown in

9

Figure 4) causes the system to oscillate if the integral gain is increased further.
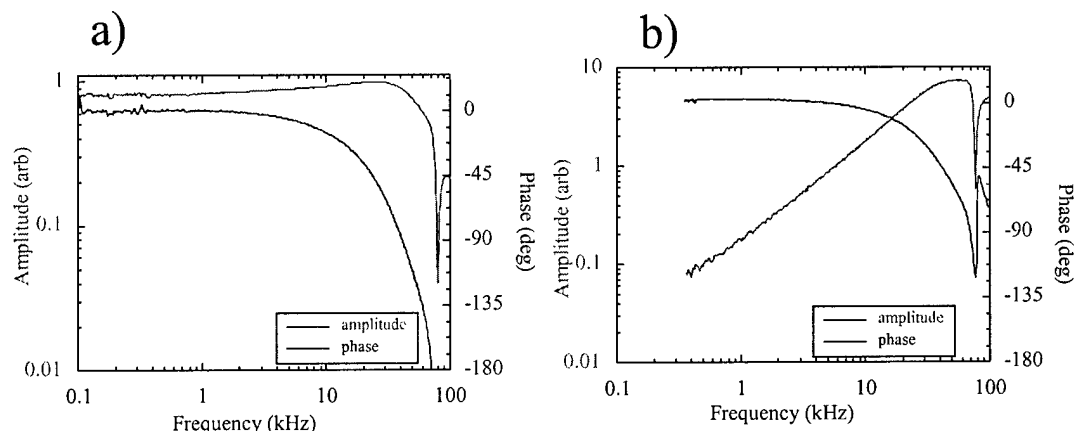

Figure 4: Frequency response of the servo loop shown in figure 2. The input to the ZnO actuator is shown in (a) and the input to the gain/integrator stages (error signal) is shown in (b). The system is driven by modulating the setpoint with a variable frequency sine wave. With a 45 degree phase margin of the error signal, the imaging bandwidth is 33 kHz. Note the mechanical resonance at 77 kHz.

Large scale imaging in the constant force mode with a tip velocity of 1 cm/s is demonstrated in Figure 5. The sample was constructed by patterning circles on a 1000 A thick gold film deposited on a Nb doped SrTiO3 substrate. Images were obtained by raster scanning the sample over an area of approximately 100 µm x 100 µm using a 2 inch long piezo tube with a fast scan rate of 50 Hz. A complete image consisting of 512 scan lines was acquired in under 15 seconds.

To circumvent resonances in the tube, the fast scan direction was driven with a sine wave while the slow scan was ramped with a triangle wave. A video acquisition system was used for the fast data acquisition. Given an x and y input, this system digitizes the z input and converts it to a video signal so that the image can be displayed on a monitor in real time. The images are then captured on video tape and downloaded to a computer for analysis.

Using the same scanning system, we reduced the scan size to the micron scale and increased the scan rate to 200 Hz. Since many frames per second could be acquired at this rate, we were able to center and zoom-in on a single feature with real time visual feedback. Figure 6 shows a section of a 1.25 µm x 1.25 µm image revealing the granular structure of the gold taken at a tip velocity of 0.5 mm/s. Although our servo loop is capable of faster tip velocities, a mechanical resonance of our piezo tube just above 200 Hz limited the scan rate. Since tip speed is a function of both scan rate and scan size, the tip speed was limited to roughly 0.5 mm/s for scan sizes on the order of 1 μm^2.

In the previous demonstration the full capabilities of the micromachined device were used in order to speed up the AFM. However, the throughput enhancements of this technique are not scaleable. The speed of the AFM in contact mode is limited by the resonance of the feedback actuator. For an actuator integrated onto a cantilever, the resonant frequency of the cantilever will scale as t/L^2 (where t is the thickness of the cantilever and L is the length of the cantilever). Unfortunately, the maximum piezoelectric induced deflection of the cantilevers[11] scales as approximately L^2/t. Using this approach, further throughput increases in AFM imaging will come at the expense of the AFMs imaging range.
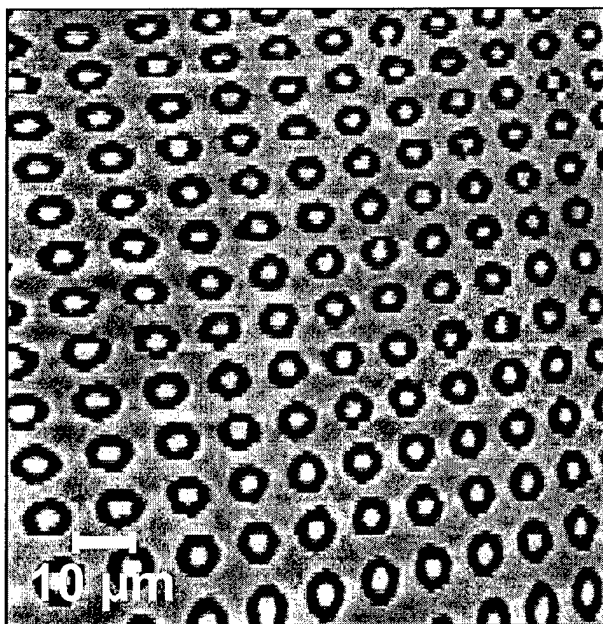
10

Figure 5: Constant force image acquired with a scan speed of 1 cm/s. The sample is made by depositing and patterning gold on a Nb-doped $SrTiO^3$ substrate. The 512 scan line image is approximately 100 x 100 um^2 and was produced in less than 15s. The image is slightly distorted due to nonlinear response of the piezotube scanner.
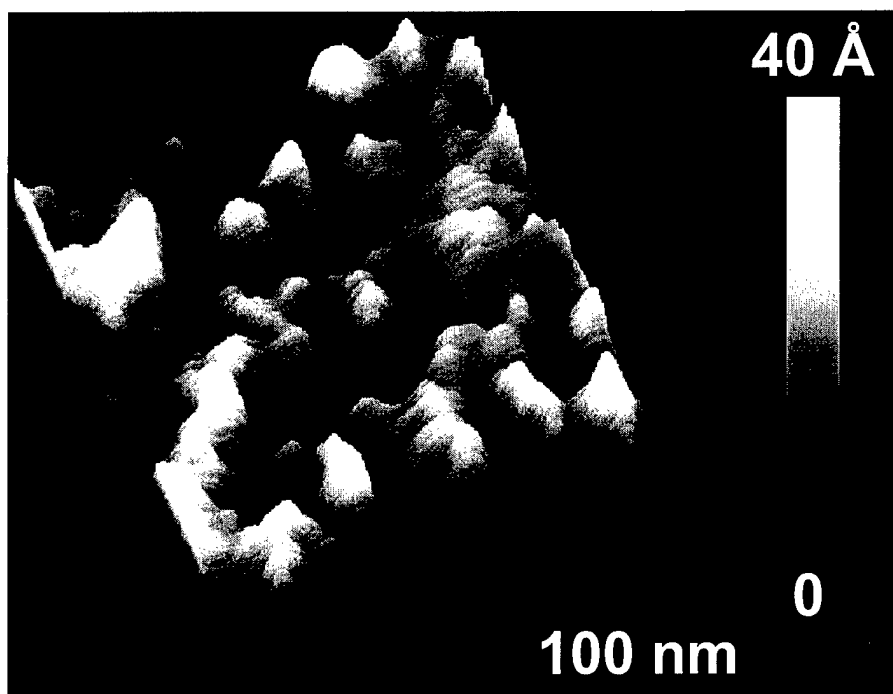
Figure 6: The granular structure of gold is evealed in this image, taken at a tip speed of 0.5 mm/s.

By simultaneously integrating a large displacement thermal actuator with a high speed piezoelectric actuator, we have shown that the speed of the AFM can be improved by over an order of magnitude without sacrificing the instrument's vertical range. This indicates that, with the appropriate sensor, the total microscope z range could be

11

increased without loss of speed, or, if the cantilever's dimensions were appropriately redesigned, the total image speed could be increased without loss of range in the z dimension. It is possible to scale this tradeoff further as only a small fraction of the thermal actuator's range is used.

It should be noted that the maximum slew rate in z is only available over the z range of the fast (piezoelectric) actuator. Thus, for example, the dual actuator will not accurately track a step greater than the range of the fast actuator. However, most sample's topographic features are microns in height with slow variation in the lateral plane, i.e., low spatial frequency. The fine features, with high spatial frequencies, have small (nm) amplitudes. The thermal actuator, with its slow response, is ideal for this situation since it can accommodate a tip displacement of several microns.
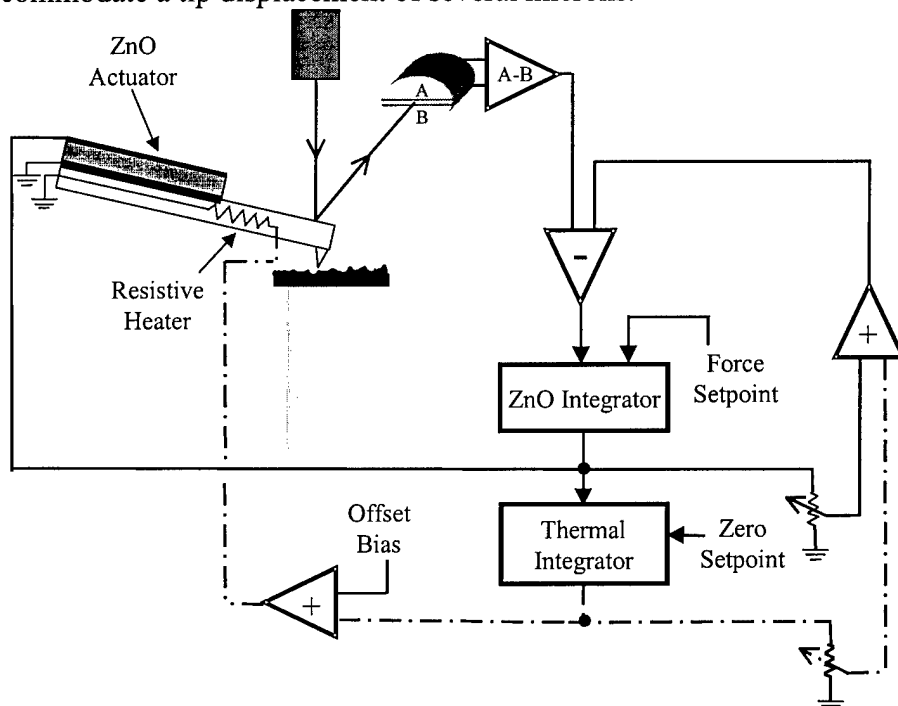

Figure 7. A schematic diagram for an AFM with integrated piezoelectric and integrated thermal actuators operating in nested feedback. The system includes two linear corrections; one to compensate for each actuator's induced angle offset. A dc bias is applied to the thermal actuator signal to ensure its value always remains positive.

Figure 7 shows a schematic diagram for implementing both the thermal and piezoelectric actuator where the deflection is monitored with the optical lever. The description and fabrication process for the cantilever used in this work is slightly different than the previous section.[12] The design presented in Figure 7 uses a nested feedback configuration which requires no filters. During operation, the fast ZnO actuator nulls the topographic signal (just as in a standard AFM), but the slower, thermal actuator responds to large scale features in topography in the attempt to keep the fast actuator's signal zero. This configuration allows the high speed actuator to stay centered within its range so that it can respond with its full displacement. The thermal actuator, on the other the hand, will maintain constant force on the slowly varying features. This is evident in the transfer function of the ZnO actuator in closed loop dual feedback operation of Fig. 8. The response of the ZnO at dc goes to zero, which means that the ZnO will not monitor

12

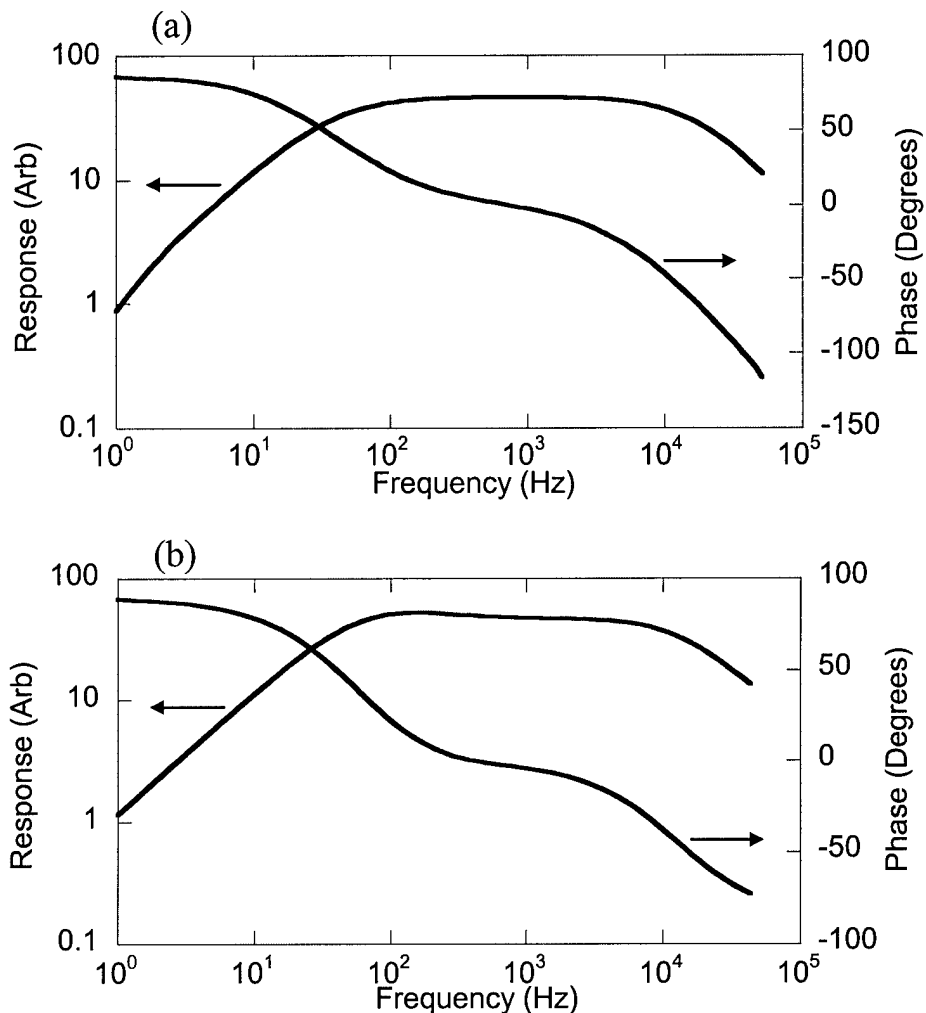the average sample position but only the high frequency data (up to 15 kHz using a 45 degree phase margin).

Figure. 8. (a) Measured and (b) simulated amplitude and phase data for the ZnO actuator in closed loop dual feedback operation. With a margin in phase of 45 degrees, the imaging bandwidth is 15 kHz. The drop-off below 60 Hz is due to the response of the thermal actuator.

Referring back to Fig. 7, it should be pointed out that both the ZnO actuator's response and the thermal actuator's response must be scaled and summed with the topographic signal. This method for correcting cantilever movement for optical detection was first reported by Manalis et. al. and has been previously described. In order to calibrate the correction circuitry, the actuators are separately modulated while the tip is free. For each actuator, the correction circuitry is adjusted until the free air deflection is nulled.

In the cantilever used for this experiment, the resistive beater for the thermal actuation consists of a p-type region implanted into n-type silicon; the resistance of the path is roughly 3 kHz. Heat is generated in the cantilever by Joule heating in the resistor, so that the different thermal expansion coefficients between silicon and ZnO create a stress throughout the bimorph which is relieved by bending.

For small applied voltages, the power follows a V^2/R relation. Vertical deflection of a cantilever bimorph is proportional to temperature, which is proportional to power,[13] and thus for low bias deflection varies with V^2. However, when the p-n junction isolation is biased beyond 12 V, we encounter p - n junction breakdown. Breakdown is seen by a sharp change in power from the quadratic dependence on applied voltage. The p - n junction after breakdown acts as a diode and clamps the voltage across the heater. A resistor placed in series with the thermal actuator, will limit the current in this breakdown region. In this regime, the power dissipated by the heater becomes proportional to the resistor controlled current. Figures 9(a) and 9(b) show the power dissipation through the heater (obtained by measuring current and applied voltage). In Fig. 9(a), a 3 kohm resistor was used in series with the thermal heater, thus showing a linear region with finite slope after breakdown. Figure 9(b) shows this effect with a 30 ohm resistor in series with the thermal heater. After breakdown, the current increases rapidly, and so therefore does the power. Operating in the breakdown region is an effective way to linearize the response of the thermal actuator. Moreover, the deflection sensitivity of the actuator can be tailored from an arbitrarily small sensitivity to a pseudobistable state simply by adjusting the series resistor.
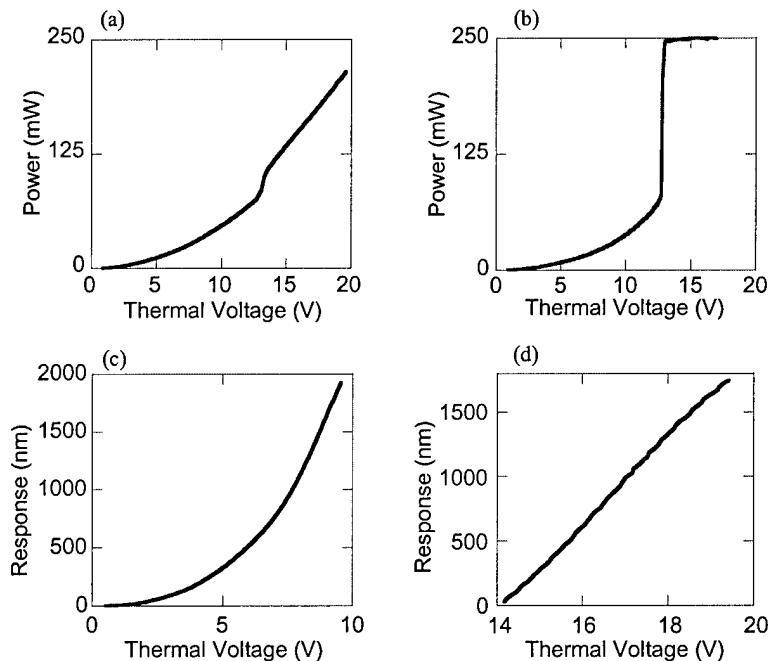

Figure 9. Thermal actuator dissipated power vs voltage ramped over time for (a) the resistive heater in series with a 3 kohm external resistor and (b) the resistive heater in series with a 30 ohm external resistor. Increasing the size of the series resistor will control and linearize the thermal actuator's deflection response in the breakdown region. Measured deflection of the cantilever is shown in the parabolic region (c) and the linear region (d).

The measured deflection curve for the thermal actuator with applied voltage below breakdown is shown in Fig. 9 (c). The quadratic voltage response of the cantilever causes the cantilever deflection to be symmetric around zero bias. Therefore, a dc offset must be applied to the thermal actuator for operation (6 V) so that voltage never drops below zero. Likewise, because the deflection response is quadratic, signal fluctuations

14

must be kept small compared to the offset bias such that displacement can be considered linear in the feedback regime. Alternatively, an integrated circuit which outputs the square root of the input can be used before the thermal actuator to linearize the response. Figure 9(d) shows the linear response of the thermal actuator in series with the 3 kohm resistor, when operated in the breakdown region.

In Fig. 10(a), we show a high speed constant force image with the dual actuators operating in the nested feedback loop. Figures 10(c) and 10(d) show the thermal and ZnO actuator signals, respectively. Figure 10(b) is the composite error signal. The image was taken with a tip velocity of 2 mm/s by raster scanning at 40 Hz over a 25 um by 25 um area. The sample came from an integrated circuit chip. Visible are metal lines and contact holes containing features over 2 um in height. In this work, the voltage applied to the ZnO was limited to ± 15 V. With this voltage range, the ZnO actuator alone is not able to deflect over the entire 2 um range of the sample, so the use of the thermal actuator increases the effective range of the high speed actuator. This 512 X512 pixel image was acquired in under 13 s. The ringing observed in the image is due to the x-y piezotube scanner and not the ZnO actuator.
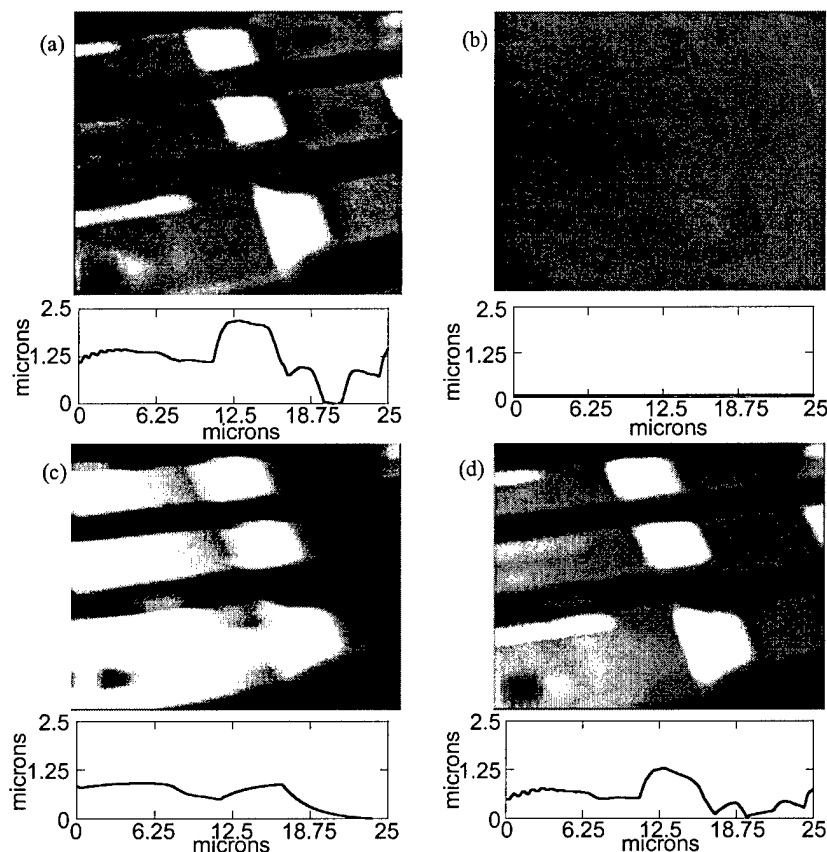
Figure 10. (a) A 512 x 512 pixel, constant force image acquired with a 2 mm/s tip velocity and dual integrated actuators. A tine profile is shown along the dotted line. (b) shows the composite error signal for the image. (c) and (d) show the thermal actuator and the ZnO actuator signals, respectively. The sample is an integrated circuit with features over 2 microns in height.

We find that neither the signal to the piezoelectric actuator nor the signal to the thermal actuator completely contain all the image topography [Figs. 10(c) and 10(d)].

15

The two signals must be appropriately combined to record the topography as shown in Fig. 10(a).

A flexible system for high speed imaging over extended ranges has been demonstrated. The feedback gain of the thermal actuator can be adjusted to either acquire the low frequency portions of the image data, or to simply remove imaging artifacts such as sample slope. It has also been demonstrated that the thermal actuator can be replaced with the standard piezotube. This may be a more appropriate way for implementing an extendible high speed system in a conventional AFM because the response of the piezotube is more linear and is better characterized.

Technical Description:
Intermittent Contact Mode Imaging

The atomic force microscope (AFM) has proven to be a useful tool for imaging a wide range of materials in a wide set of environments. Intermittent contact mode, or tapping mode, imaging was first introduced by Zhong et. al.[14] It has become the dominant mode of AFM imaging because it reduces lateral forces between the tip and sample.[15]

The cantilever driven at its resonant frequency will achieve a free air amplitude determined by the drive amplitude, the spring constant, and the quality factor of the cantilever's resonance (Q). As the cantilever is brought into contact with the sample, the surface will limit the oscillatory motion. The amplitude is typically 10 to 100 nm and is measured with a split photodetector. The RMS amplitude of the cantilever is kept constant with a feedback loop that controls the vertical distance between the tip and the sample. In most AFMs, the feedback loop controls a conventional piezotube such that when the sample topography causes the cantilever's RMS amplitude to change, the piezotube will extend or contract to restore the cantilever's original RMS value.

While the tapping mode AFM allows nanometer scale resolution with negligible frictional forces, it is encumbered by slow imaging speed. The scan speed of typical tapping mode AFMs is limited in part by the resonant frequency of the piezotube and in part by the time it takes for the oscillating cantilever to change amplitude. (Other factors play a role in the tapping mode imaging speed, such as the bandwidth of the RMS to DC converter, but these are secondary). For most samples, these constraints limit the tapping mode AFM's scan speed to a few tens of microns per second. At this speed a single, moderately sized 512×512 pixel image will take several minutes to acquire.

We have increased the tapping mode imaging rate with two improvements. First, and as before, a faster z-axis actuator is integrated onto the cantilever. Second, an active damping circuit is applied to increase the speed at which the cantilever can respond.

In other approaches for high speed tapping mode imaging, Paloczi et. al.[16] have taken advantage of the low Q and high resonant frequency of small cantilevers in liquid to image with scan speeds of 52 μm/s without the use of feedback. Ookubo et. al.[17] obtained a 225 μm/s speed by combining the feedback signal and the error signal into a composite topographic signal. This method can indeed increase speed, but it does so at the expense of increased tip/sample force.

Here, we use the zinc oxide (ZnO) piezoelectric actuator to both drive the cantilever at its resonant frequency and to provide z actuation. The cantilever is the same

as the one used in the dual actuator contact configuration. In Figure 11 we compare the response of the integrated ZnO actuator with that of a typical piezotube actuator.[18] The resonant frequency of the z-actuator marks the point of 180 degree phase shift with the drive (90 degrees at the resonant frequency and 90 degrees from the feedback integrator). To avoid instability the maximum gain of the feedback loop is limited such that the response at this frequency is less than one. Therefore the z-actuator's resonant frequency sets an upper limit on imaging bandwidth. The addition of the integrated ZnO actuator increases the resonant frequency by nearly a factor of 40 over the piezotube.
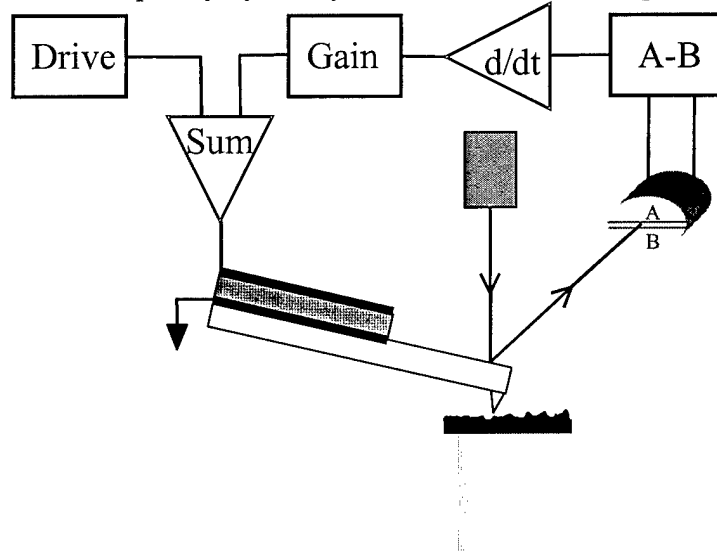

Figure 11: Amplitude response of a ZnO cantilever and a conventional piezotube. The mechanical response of the ZnO is 40 times faster than that of the piezotube.

In tapping mode, the scanning speed is additionally constrained by 1) a small maximum error signal which limits the feedback's output, and 2) the cantilever's high Q which results in long time constants for changes in error signal. The error signal is defined as the setpoint, a_{SP} (the desired tapping amplitude), minus the RMS amplitude, a_{RMS} (the actual tapping amplitude). Typically, the setpoint is chosen to be slightly below the free air amplitude of the cantilever. This ensures that the tip is tapping lightly on the sample. A property of tapping mode that limits the speed is the magnitude of the error signal. For accurate imaging the signal should be proportional to the change in topography, but this is not always true. For the case where the tip encounters a sufficiently large upward step, the cantilever's amplitude will decrease until the oscillation is completely quenched. After this the error signal becomes saturated at a_{SP}. If the sample contains a sharp downward step, the sample will no longer impede the oscillation, and the cantilever amplitude will increase and saturate at the free air amplitude, a_{free}.

Since the setpoint is generally chosen to be close to the free air amplitude, the maximum error signal on a downward step is necessarily small. This limited error signal constrains the feedback loop to a slow response (in comparison to an upward step). In general, the speed of tapping mode imaging can be increased by simply using a smaller

setpoint since this allows a larger error signal. However, this strategy requires a stronger tapping force which is undesirable.

When scanning over a downward step, a cantilever initially operating with an amplitude of a_{SP} (an error signal of zero), will ring up to a maximum amplitude of a_{free} (a negative error signal of $a_{SP} - a_{free}$). The Q of an oscillating system is defined as 2π times the mean stored energy divided by the work per cycle.[19] For a high Q cantilever driven at resonance, the error signal during a transient (resulting from a step) follows an exponential path with a time constant inversely proportional to Q. The tapping mode error signal will be delayed in response as the error signal grows to an appreciable value. For a cantilever system with a Q of several hundred and a resonant frequency of 100 kilohertz, this ring-up can take more than a millisecond. In order to achieve nanometer resolution on samples with sharp features, this delay will limit the scan speed to a few microns per second.

Our solution to this problem is to use active damping to change the cantilever's apparent Q. Mertz et. al.[20] developed a system for actively damping an AFM cantilever to speed up the system's mechanical transients. Their system used a thermal bimorph actuator to apply the active control. Garbini et. al.[21] extended this work by designing a controller for active modification of cantilever dynamics to improve the stability of magnetic force microscopy. Bruland et. al.[22] used a similar control system to actively control an ultrasoft magnetic cantilever with an external field.

Our active damping is accomplished with a feedback circuit. We can understand this technique by examining the equation of motion for the oscillating cantilever: $F = m\ddot{z} + b\dot{z} + kz$ where m is mass, z is deflection, b is damping factor, k is spring constant, and F is the cantilever drive. The derivatives are with respect to time. Q is inversely proportional to the damping factor, b. For active damping of this system, we use the ZnO actuator to add a force that is proportional to the velocity of the cantilever for frequencies in the imaging bandwidth. The AFM measures the deflection of the cantilever, z, and thus is converted to velocity, $\dot{z}$, with an electronic differentiator or phase shifter. We then add this signal back into the drive to gain full control over the Q, and the transient response.

Trace (a) in Figure 12 shows the amplitude and phase response of a ZnO cantilever at resonance with a resonant frequency of 46 kHz and a Q of 150. In trace (b), we show the response is damped by a factor of 20. Active damping allows the cantilever to reach its free air amplitude faster, and this reduces the delay associated with cantilever ring up. The ZnO cantilever is uniquely suited for active damping when compared to the response of a typical cantilever driven by a piezoslab shown in trace (c). In most AFMs, cantilevers are excited with a piezoslab located on a cantilever holder. The mechanical connection in this arrangement creates spurious responses for both amplitude and phase. These deviations from the ideal system make it difficult to stabilize and maintain active control.

In Figure 13 we show the effect of active control on the cantilever ring-up time. There we display the error signal versus time when the cantilever suddenly loses contact with the surface. These results were obtained by tapping on a bare silicon sample that was quickly retracted at t = 0.[23] In Figure 13, trace (b) is the error signal for a cantilever with no active control. Reducing the apparent Q by a factor of two with active damping produces the faster ring up time shown in trace (a). We can also increase the apparent Q

18

by reversing the gain of the active damping circuit. Trace (c) shows the slower response when the Q is increased by a factor of two (although the increased Q slows down imaging, it is useful to increase the range of the attractive regime[24]). We extracted the change in the apparent value of Q by fitting the error signal to an exponential. All of the Q values are smaller than those observed in free air, but correspond to Q measurements taken at 100nm above the surface. This decrease in Q when close to the surface is due to squeeze film damping between the cantilever and the sample.[25]
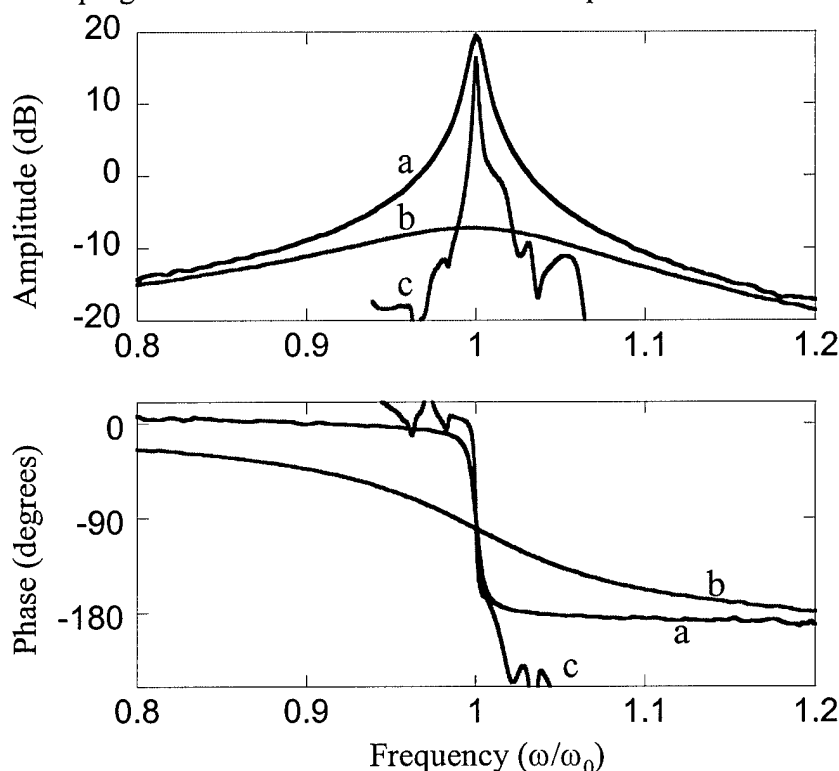

Figure 12: Amplitude and phase responses of a ZnO cantilever and a commercial Si cantilever. The frequency axis has been normalized in units of ω_0. Traces (a) and (b) show the resonance of the ZnO cantilever and the ZnO cantilever with active damping respectively. In this case, the cantilever is damped from a Q of 150 to a Q of 7. Trace (c) shows a typical resonance of a silicon cantilever driven with a commercial piezoslab. Because the actuator is external to the cantilever, the amplitude and phase show significant deviation from an ideal second order response. This is particularly a problem if Q damping is attempted.

In Figure 14 we show an image and a line trace of a grating taken with both the standard tapping mode system (a), and with the ZnO cantilever under active control (b). Both images were taken with a scan rate of 5 Hz, with equal tapping amplitudes, setpoints, and optimized gains. The image taken with the piezotube as the z-axis actuator does not follow topography, and tends to become unstable when changes in height were encountered. However, the scan with the actively damped ZnO cantilever faithfully reproduces the sample topography. This is evident from the line traces. Figure 14c shows a 2.4 mm/s image of a laser textured landing zone on a hard disk using both the fast ZnO actuator and active damping.

By combining the benefits of a fast z-axis actuator and active control of the cantilever dynamics, we can increase the speed and decrease the recording time for

19

tapping mode images by more than an order of magnitude. Images of smaller size could be acquired faster, which will allow for fast, real-time imaging.
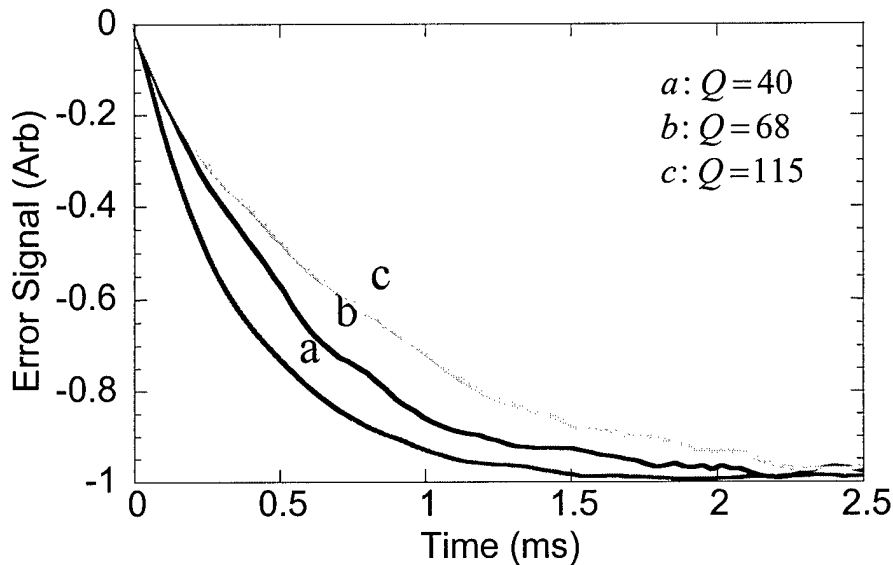

Figure 13: The traces show the error signal versus time when the cantilever suddenly loses contact with a surface. Trace (b) is the error signal for a cantilever with no active control. The resonance in trace (a) is damped by a factor of 2. The resonance in trace (c) is enhanced by a factor of 2. These curves were fit to an exponential and solved for Q.

Estimates of Technical Feasibility

The research carried out under this contract provides a sound base for the commercialization of a very high speed atomic force microscope based on a MEMS cantilever with an integrated actuator and specialized circuitry. Typical microscopes scan at tens to hundreds of microns per second. We have demonstrated scan speeds of up to a centimeter per second. This speed advance changes the whole look and feel of the AFM from a research tool that takes hours of use to obtain final data, to a tool that images in real time with scan and zoom capabilities. This will both change the how the AFM is perceived for high throughput manufacturing applications as well as open new doors for short time scale research applications. The high speed AFM is technically feasible. Further research is needed to understand the effects of high speed imaging on resolution, linearity, and tip wear. These topics will be the focus of the Phase II proposal.
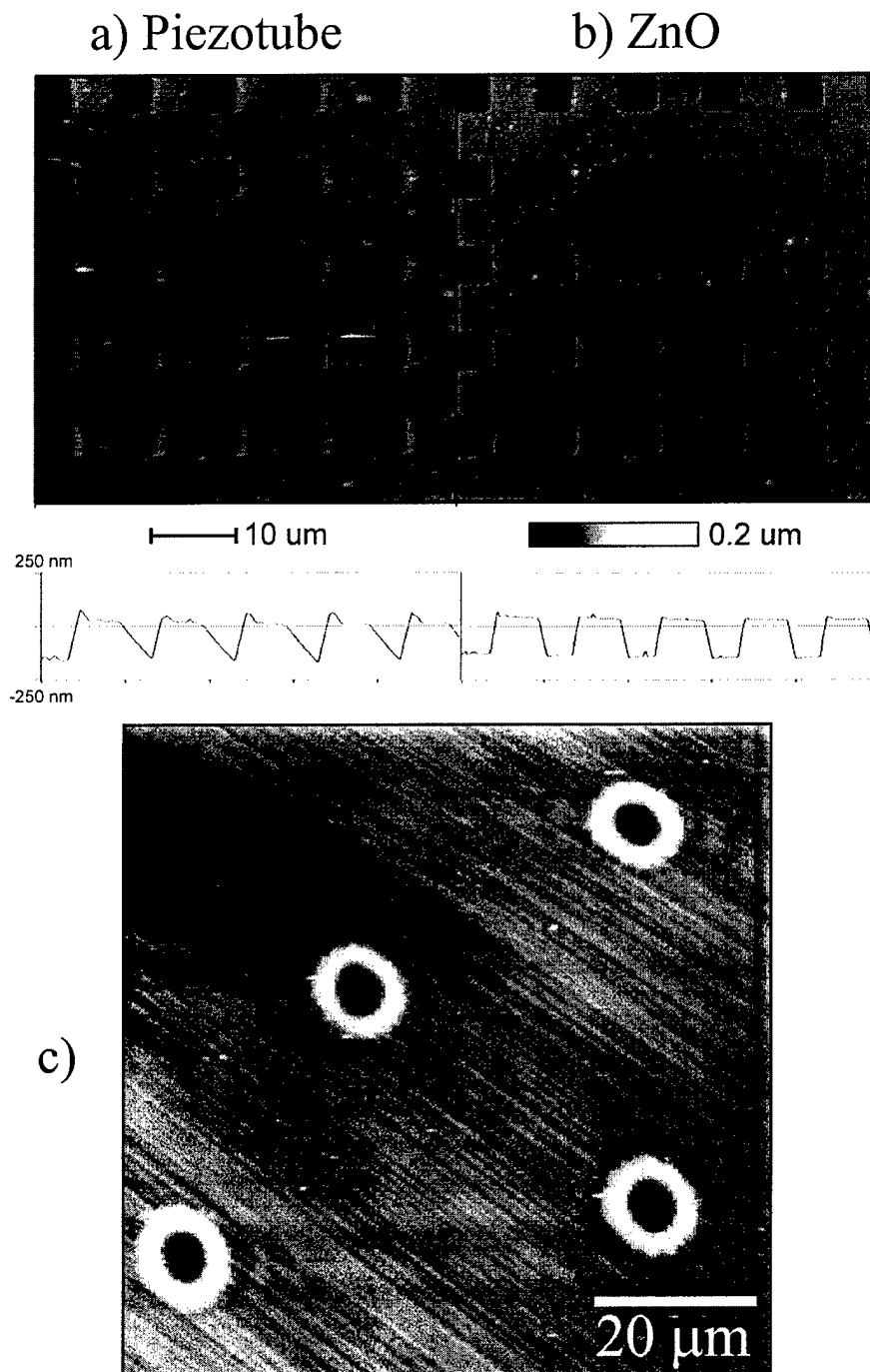
20

Figure 14: (a) and (b) show images of a grating taken at a 5 Hz scan rate with equal tapping amplitudes, setpoints, and optimized gains. The z actuator in (a) is a piezotube and in (b) is an actively damped ZnO cantilever. The line traces shows the piezotube's inability to effectively follow topography at these speeds. (c) shows an image of a hard drive disk using both fast ZnO actuator and active damping. The image scan size is 80 microns and the scan rate is 15 Hz, putting the imaging speed at 2.4 mm/s. This high resolution image reveals the polishing of the disk and the laser zone texturing and has a z range of 80 nm. The image was taken in just over 17 seconds. The image has been filtered to remove the vertical resonances of the xy scanner caused when driven at a high rate.

Future Plans

We plan to continue to advance the state of the art in high speed atomic force microscopy through further cantilever, microscope, and electronic innovation. We are in the process of applying for a Phase II proposal. We are currently in negotiation with Digital Instruments of Santa Barbara, CA to providing matching funds for a Fast Track Effort.

Contract Delivery Status

There are two deliverables of this contract: 1) the quartley status report, and 2) this final report.

1) DI-MGMT-80368 Status Report, Sequence A001, Due 02/08/00, Submitted and Accepted on time.
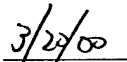2) DI-MISC-80711, Scientific and Technical Final Report, Sequence A002, Due 06/30/00, Submitted on time.

Report Prepared By

Stephen C. Minne, Ph.D.
NanoDevices Inc.
516 E. Gutierrez, Suite E
Santa Barbara, CA 93103
805-884-0240
805-884-0540 (fax)
steve@ndevices.com

Appendix I:
Declaration of Technical Data Conformity

The contractor, NanoDevices Inc., hereby declares that, to the best of its knowledge and belief, the technical data delivered herewith under contract No. DAAH01-00-C-R014 is complete, accurate, and complies with all requirements of the contract.

Stephen C. Minne, Ph.D.   Date
President, NanoDevices, Inc.

Appendix II:
Distribution List

Commander   2 Copies
U.S. Army Aviation and Missile Command
ATTN: AMSAM-RD-WS-DP-SB
(Mr. Alexander H. Roach, Technical Monitor)
Bldg. 7804, Room 205
Redstone Arsenal, AL 35898

Commander   1 Copy
U.S. Army Aviation and Missile Command
ATTN: AMSAM-RD-OB-R
Bldg. 4484, Room 204
Redstone Arsenal, AL 35898-5241

Commander   1 Copy
U.S. Army Aviation and Missile Command
ATTN: AMSAM-RD-WS
Bldg. 7804, Room 247
Redstone Arsenal, AL 35898-5248

Director   1 Copy
Defense Advanced Research Projects Agency
ATTN: MTO (Dr. Christie R. K. Marrian)
3701 North Fairfax Drive
Arlington, VA 22203-1714

Director   1 Copy
Defense Advanced Research Projects Agency
ATTN: ASBD/DARPA
3701 North Fairfax Drive
Arlington, VA 22203-1714

Director   1 Copy
Defense Advanced Research Projects Agency
ATTN: ASBD/DARPA Library
3701 North Fairfax Drive
Arlington, VA 22203-1714

Defense Technical Information Center   2 Copy
ATTN: Acquisitions/DTIC-OCP, Rm-815
8725 John J. Kingman Rd., STE 0944
Ft. Belvoir, VA 22060-6218

Endnotes

1 R. C. Barett, C.F. Quate, J. Vac. Sci. Technol. B 9, 302 (1991).

2 H. J. Mamin, H. Birk, P. Wimmer, D. Rugar, J. Appl. Phys. 75, 161 (1994).

3 S. C. Minne, H. T. Soh, Ph. Flueckiger, and C. F. Quate, Appl. Phys.   Lett. 6, 703 (1995).

4 S. C. Minne, Ph. Flueckiger, H. T. Soh, C. F. Quate, J. Vac. Sci.   Technol. B 13, 1380 (1995).

5 S.R. Manalis, S.C. Minne, and C.F. Quate, Appl. Phys. Lett. 68, 871 (1995).

6 S.R. Manalis; S.C. Minne; A. Atalar; C.F. Quate, Rev. Sci. Instrum. **67**, 3294 (1996).

7 G. Meyer and N.M. Amer, Appl. Phys. Lett. 53, 1045 (1988).

8 S. Alexander, L. Hellemans, O. Marti, J. Schneir, V. Elings, P.K. Hanmsa, M. Longmire, and J. Gurley, Appl. Phys. Lett. 65, 164   (1989).

9 T. Fujii and S. Watanabe, Appl. Phys. Lett. 68, 467 (1996).

10 S.C. Minne, S.R. Manalis, C.F. Quate, Appl. Phys. Lett. 67, 3918 (1995)

11 J.G. Smits; W.S. Choi, Proceedings of the 1994 IEEE International Frequency Control Symposium, 139, (1994).

12 S.C. Minne; G. Yaralioglu; S.R. Manalis; J.D. Adams; J. Zesch, A. Atalar; C.F. Quate, Appl. Phys. Lett., **72**, 2340 (1998).

13 J. R. Barnes, R. J. Stephenson, C. N. Woodburn, S. J. O'Shea, M. E. Welland, T. Rayment, J. K. Gimzewski, and Ch. Gerber, Rev. Sct. Instrum. **65**, 3793 (1994)

14 Q. Zhong, D. Imniss, K. Kjoller, and V. B. Elings, Surf. Sci. **290**, L688 (1993).

15 S. H. Leuba, G. Yang, C. Robert, B. Samori, K. van Holde, J. Zlatanova, and C. Bustamante, Proc. Natl. Acad. Sci. USA **91**, 11 621 (1994).

16 George T. Paloczi, Bettye L. Smith, Paul K. Hansma, Deron A. Walters, and Mark A. Wendman, Appl. Phys. Lett. **73**, 1658 (1998).

17 Norio Ookubo and Seiji Yumoto, Appl. Phys. Lett. **74**, 2149 (1999).

18 Dimension 3000, Digital Instruments, Santa Barbara, CA 93117.

19 Richard Feynman, The Feynman Lectures on Physics Vol. 1, p. 24-2

20 J. Mertz, O. Marti, and J. Mlynek, Appl. Phys. Lett. **62**, 2344 (1993).

21 J L. Garbini, K.J. Bruland, W.M. Dougherty, and J.A. Sidles, J. Appl. Phys. **80**, 1951 (1996).

22 K.J. Bruland, J.L. Garbini, W.M. Dougherty, and J.A. Sidles, J. Appl. Phys. **83**, 3972 (1998).

23 This exponential increase in error signal is also observed when imaging downward steps.

24 B. Anczykowski, J.P. Cleveland, D. Kruger, V. Elings, H. Fuchs Appl. Phys. A **66**, S885 (1998).

25 F.M. Serry, P. Veuzil, R. Vilasuso, and G.J. Maclay, Proceedings of the Second International Symposium on Microstructures and Microfabricated Systems, Chicago (Second International Symposium on Microstructures and Microfabricated Systems, 1995), p. 83.